Covalently Tethered Comb-Like Polymer Brushes on Hydrogen-Terminated Si (100) Surface via Consecutive Aqueous Atom Transfer Radical Polymerization of Methacrylates

Guangqun Zhai, Y. Cao, J. Gao

Department of Materials Science and Engineering, Jiangsu Polytechic University, Changzhou 213016, People's Republic of China

Received 13 February 2006; accepted 26 April 2006
DOI 10.1002/app.24698
Published online in Wiley InterScience (www.interscience.wiley.com).

ABSTRACT: The hydrogen-terminated Si (100) (Si—H surface) was functionalized by coupling with 4-vinylbenzyl chloride (VBC) to form a Si—VBC surface, which serves as macroinitiators for the surface-initiated aqueous atom transfer radical polymerization (ATRP) of 2-hydroxyethyl methacrylate (HEMA) and poly(ethylene glycol)methacrylate (PEGMA) to prepare Si—VBC—*g*—PHEMA and Si—VBC—*g*—PPEGMA substrates, respectively. The ellipsometric results revealed that the surface-initiated ATRP of both PHEMA and PPEGMA brushes proceeded in a controlled fashion. By adjusting the monomer concentration, an eccentric polymer thickness dependence on the initial monomer concentration $[M]_0$ was observed for both HEMA and PEGMA, i.e., in the dilute regime, the thickness of the polymer film increases with the increase in $[M]_0$; however, beyond critical $[M]_0$, the thickness deceases gradually with the further increase. Such an eccentricity was tentatively correlated to the counteractive combination of the increase in $[M]_0$ and decrease in the apparent polymerization rate constant. Both Si—VBC—*g*—PHEMA and Si—VBC—*g*—PPEGMA substrates were esterified for the subsequent surface-initiated ATRP, resulting in corresponding comb-like brushes. © 2006 Wiley Periodicals, Inc. J Appl Polym Sci 102: 2590–2599, 2006

Key words: atom transfer radical polymerization; branched; ESCA/XPS; esterification; interface

INTRODUCTION

Polymer brushes refer to polymer chains tethered on a substrate surface in a fairly well-defined conformation.[1,2] Physical adsorption is a facile approach to form polymer brushes for end-functional polymers, which can adsorb on the substrate surface via hydrophilic–hydrophobic interaction, hydrogen-bonding, or electrostatic interaction. However, the noncovalent nature of these interactions is responsible for the inconsistent performance of the polymer brushes.[1,2] Accordingly, the chemical approaches, viz., the *grafting to* and *grafting from* approaches, have been advanced to circumvent such drawbacks. The *grafting to* approach is directed to the immobilization of the existing end-functionalized polymer chains onto the pretreated substrate surface via the classic organic reactions. Nonetheless, the efforts to prepare polymer brushes in high density went in vain due to steric hindrance. The *grafting from* technique involves the immobilization of initiator moieties on the substrate surface initially, followed by the surface initiated polymerization to introduce the polymer chains onto the substrate surface. There have been a great deal of reports on the syntheses of polymer brushes via the surface-initiated conventional radical polymerization,[3,4] anionic living polymerization,[5,6] ring-opening polymerization,[7,8] and group transfer polymerization[9] to produce the linear polymers.

Research on controlled radical polymerizations (CRPs), especially atom transfer radical polymerization (ATRP), has enjoyed a rapid growth since the late 1990s.[10–12] Since the first report,[13] ATRP has also been widely adopted in the syntheses of polymer brushes on a variety of substrate surfaces. For example, the functionalized thiol (C—SH) can be adsorbed on the gold nanoparticles, and ATRP can be initiated from the surface-bound C—Br moieties to form the polymer brushes.[14–16] The silanol group (Si—OH) on the silica surface, on the other hand, can be functionalized by silane coupling agents, containing C—Cl or C—Br groups, initiator moieties for ATRP.[17,18] For the silicon substrates with the transformed Si—H surface, initiator moieties for ATRP can be introduced onto such surfaces via the L-B technique[13,19] or the photochemical approach.[20] On the other hand, organic compounds,

Correspondence to: G. Q. Zhai (zhai_gq@hotmail.com).
Contract grant sponsor: Natural Science Foundation of China; contract grant number: 20574033.
Contract grant sponsor: Natural Science Foundation of Jiangsu Province; contract grant number: BK2005404.

such as polystyrene latex particles, were also used as the substrates for the surface-initiated ATRP, leading to a hydrophilic shell and a hydrophobic latex core.[21] Because the end-functionality of the polymer brushes from the ATRP process could function as a surface-bound macroinitiator in the subsequent reaction, block copolymer brushes can be easily prepared through the consecutive monomer addition. Therefore, the surface-initiated ATRP process can readily lead to the linear copolymer brushes.[22]

There also have been reports on the synthesis of polymer brushes with a branched architecture via CRPs. For example, hyperbranched polymer brushes can be produced from the initiator-monomer, or AB* *inimer* (A, polymerizable double bond; B*, initiating group).[23,24] Acrylic acid (AAc)-based dendritic polymer brushes have also been reported via the repeated *grafting to* strategy of amine-terminated poly(*tert*-butyl acrylate) (NH_2—P(*t*-BA)—NH_2) on the carboxylic acid-terminated solid substrate.[25] Another strategy to *graft* dendritic PAAc brushes to the solid substrate involves the immobilization amine-containing siloxyl coupling agent on the glass bead surface, followed by the amidization of amine group with carboxylic acid.[26] However, few attempts have been reported on the preparation of regularly grafted, or comb-like, polymer brushes on inorganic substrates.

In the present work, comb-like polymer-silicon hybrids were prepared via consecutive surface-initiated ATRP on the hydrogen-terminated Si 100 substrates (Si—H surface). UV-induced coupling of 4-vinylbenzyl chloride with the Si—H surface resulted in the immobilization of an ATRP initiator layer on the Si surface, followed by ATRP of hydroxyl-containing methacrylates to give rise to functional linear polymer brushes. The hydroxyl groups alongside the brushes were esterified to introduce the C—Br moieties. Comb-like polymer brushes were subsequently synthesized in the second round of ATRP. Such a process may provide a facile protocol for the preparation of branched and arborescent polymer brushes on solid substrates from the hydroxyl-functional monomers via consecutive ATRP.

EXPERIMENTAL

Materials

Poly(ethylene glycol)methacryate (PEGMA) (MW = 360), 2-hydroxyethyl methacrylate (HEMA), and 4-vinylbenzyl chloride (VBC) were purchased from Aldrich Chemical Company of Milwaukee, WI, and the inhibitors were removed by column chromatography before use. (100)-oriented single crystal silicon wafers, or Si (100) wafers, with a thickness of about 0.7 mm and a diameter of 150 mm, were obtained from Unisil of Santa Clara, CA. It was sliced into rectangular strips of about 1×3 cm^2 in size. The silicon wafer was pretreated with HF to remove the native oxide layer and to result in a hydrogen-terminated silicon surface (the Si—H surface), following the procedures described in literature.[20] The catalysts, copper (I) chloride (CuCl) and copper (II) chloride ($CuCl_2$), the ligand for the ATRP, bipyridine (bPy), and 2-bromoisobutylryl bromide was also from Aldrich Chemical. They were used as received.

Surface modification

Immobilization of the ATRP initiator moiety

For the Si—H substrate, the ATRP initiator moiety was introduced by coupling VBC to result in a Si—VBC substrate on a Riko RH400-10W rotary photochemical reactor (manufactured by Riko Denki Kogyo of Chiba, Japan), as shown in Figure 1.[27]

Synthesis of the PHEMA and PPEGMA brushes on the silicon surface

PHEMA and PPEGMA brushes were prepared on Si—VBC. HEMA or PEGMA monomer, as well as the

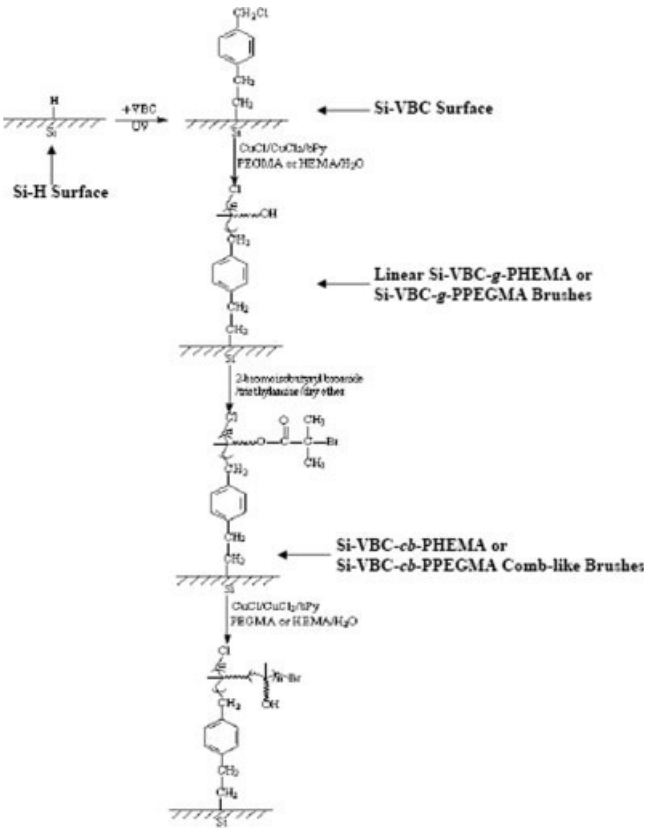

Figure 1 Schematic illustration of the immobilization of VBC on Si—H substrate, the surface-initiated ATRP of HEMA and PEGMA on Si—VBC substrate, the esterification of Si—VBC—*g*—PHEMA and Si—VBC—*g*—PPEGMA substrate, and the synthesis of comb-like PHEMA and PPEGMA brushes.

doubly distilled water, was added to a test tube equipped with a magnetic stirring bar, to achieve a total volume of 15 mL and a specific vol/vol concentration. As a typical process, 6 mL of HEMA (about 0.05 mol) and 9 mL double distilled water were added into the test tube to achieve a specific vol/vol concentration of 0.4. 30 mg of CuCl (0.30 mmol), 8 mg of $CuCl_2$ (0.06 mmol), and 112 mg of 2,2′-bipyridyl (bPy, 0.72 mmol) were added to the mixture under stirring. The solution was degassed by a stream of purified argon for about 20 min. A piece of the pretreated silicon substrate was added into the solution. The solution was sealed and left to react at room temperature for a predetermined period of time. After the reaction, the silicon strip was ultrasonicated for 2 min and washed in copious ethanol and doubly distilled water repeatedly, and was dried by pumping under reduced pressure. The processes of surface-initiated ATRP of HEMA and PEGMA are also illustrated schematically in Figure 1.

Functionalization of the PHEMA and PPEGMA brushes

Si—VBC—*g*—PHEMA and Si—VBC—*g*—PPEGMA substrates were functionalized to introduce the ATRP initiator moieties, under the similar conditions as described in the literature.[20] The esterification of hydroxyl groups of the PHEMA and PPEGMA brushes was carried out with the 2-bromoisobutyryl bromide, leading to the Si—VBC—*g*—PHEMA—Br and Si—VBC—*g*—PPEGMA—Br substrates, respectively, which could serve as surface-bonded ATRP macroinitiators. This strategy is illustrated schematically in Figure 1.

Synthesis of comb-like PHEMA and PPEGMA brushes via divergent ATRP

The preparation of comb-like polymer brushes was carried out in a similar approach as that of linear analogue, except that Si—VBC—*g*—PHEMA—Br and Si—VBC—*g*—PPEGMA—Br substrated were used instead of Si—VBC, respectively, as shown in Figure 1.

Surface characterization

The surface composition and chemical states of the silicon substrates were measured by X-ray photoelectron spectroscopy (XPS). XPS measurements were carried out on a Kratos AXIS HSi spectrometer, under the similar conditions as those reported before.[20] The topography of the silicon substrates was probed by atomic force microscopy (AFM), using a Nanoscope IIIa AFM from the Digital Instrument, and the thickness of polymer film thickness was determined on a variable angle spectroscopic ellipsometry (Model VASE®, J. A. Woollam Lincoln, NE), under the similar conditions as reported before.[20]

Static water contact-angle goniometry of the various substrates was carried out on at room temperature and 60% relative humidity by the sessile drop method, using a 3-μL water droplet in a telescopic goniometer (Rame-Hart, Model 100-00-(230), manufactured by the Rame-Hart of Mountain Lakes, NJ). The telescope with a magnification power of 23× was equipped with a protractor of 1° graduation. For each sample, the measurements were made on at least three different surface locations and the results were averaged. Each contact angle reported was reliable to ±3°.

RESULTS AND DISCUSSION

Surface hydrosilylation of VBC

Hydrosilylation, or the addition of the Si—H moiety to the unsaturated C=C double bond, has been widely reported.[28,29] In fact, the surface hydrosilylation of the hydrogen-terminated silicon substrate (Si—H surface) has recently been reviewed.[30] In this study, the ATRP

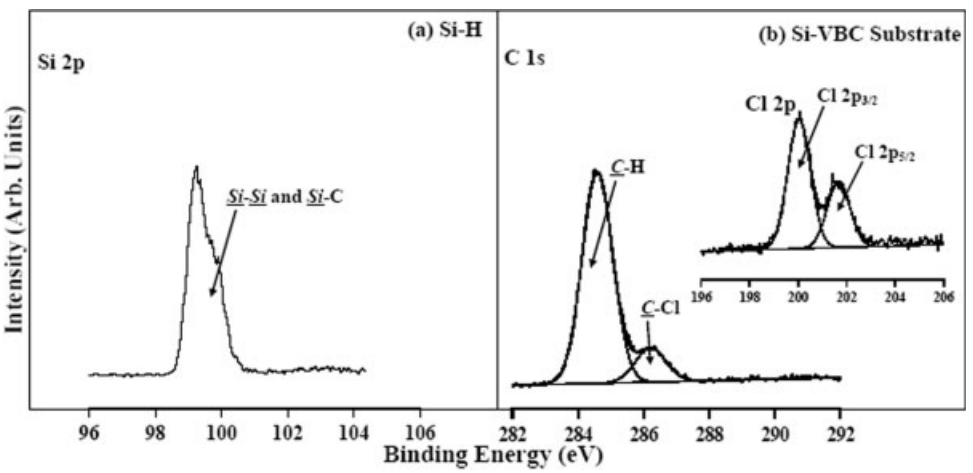

Figure 2 (a) XPS Si 2p core-level spectrum of Si—H substrate; (b) C 1s and Cl 2p core-level spectra of the Si—VBC substrate.

TABLE I
Surface Properties of the Si—VBC, Si—VBC—PHEMA, and Si—VBC—PPEGMA Substrates

Surface	Polymerization time (h)	Water contact angle (±3°)	Thickness (+1 nm)	$([C—Cl] : [C—H])_{surface}$ or $([CH_2] : [C—O] : [C=O])_{surface}$ ratio[a]	Surface roughness (nm)[b]
Si—VBC	0	87	2.2	0.16	0.18
Si—VBC—*g*—PHEMA[c]	4	44	26.8	3.67 : 1.65 : 1	0.74
Si—VBC—g—PPEGMA[b]	4	46	56.1	6.75 : 10.62 : 1	1.50

[a] Determined from XPR spectral area ratio; $([C—Cl] : [C—H])_{surface}$ for Si—VBC and $([CH_2] : [C—O] : [C=O])_{surface}$ for Si—VBC—*g*—PHEMA and Si—VBC—*g*—PPEGMA surfaces.
[b] Determined from the AFM.
[c] Prepared from Si—VBC, conditions: monomer concentration, 0.27 (v/v); reaction time, 4 h at room temperature.
[d] Prepared from Si—VBC, conditions: monomer concentration, 0.40 (v/v); reaction time, 4 h at room temperature.

initiator was introduced, via the surface hydrosilylation of an inimer, VBC, under UV irradiation, on the Si—H surface to produce the Si—VBC surface. The surface chemical composition and topography of the Si—VBC substrate were analyzed by XPS and AFM, respectively.

Figure 2(a) shows the XPS Si 2p core-level spectrum of Si—H surface. The Si 2p peak with binding energy (BE) at about 99 eV was assigned to the Si—Si species.[31] The peak component associated with the Si—O species, with BE at about 103 eV, has almost completely disappeared.[20,31] The XPS result suggested that after the pretreatment of hydrofluoric acid solution, the native oxide layer has been removed to give rise to a hydrogen-terminated silicon surface (Si—H surface).

Figure 2(b) shows the C 1s and Cl 2p core-level spectra of the Si—VBC substrates. The C 1s core-level lineshape of the Si—VBC substrate was curve-fitted with two peak components. The peak components with the binding energies (BE's) at 284.6 eV and 286.2 eV were assigned to the *C*—H and *C*—Cl species of VBC, respectively.[31] The π–π^* shake-up satellite of the VBC is also discernible at the BE of about 290.4 eV.[31] The ratio of the *C*—Cl moiety to the *C*—H species, as determined from their respective peak component area ratio, is estimated to be about 0.16, which is slightly higher than the theoretical value of 0.12 of the VBC monomer. The Cl 2p core-level lineshape was resolved into Cl $2p_{3/2}$ and Cl $2p_{5/2}$ peak components with a separation energy of 1.33 eV.[31] XPS results are thus consistent with the presence of immobilized VBC on the Si—H surfaces.

Although it has been assumed that surface hydrosilylation of VBC on the Si—H substrate leads to a molecular monolayer, evidences indicated that a VBC oligomer layer probably has formed instead. The surface $([Cl]/[C])_{surface}$ ratio, as determined from their respective core-level spectral peak area, is about 0.06, significantly less than the theoretical value of 0.11 for the VBC monolayer. Furthermore, as shown in Table I, the thickness of the VBC monolayer on the Si—VBC substrate was determined by ellipsometry to be about 2 nm. Telomerization of VBC may have occurred under the UV induction. The Si—H moiety undergoes the homolytic cleavage to produce the surface radicals that initiated the oligomerization of VBC to produce the

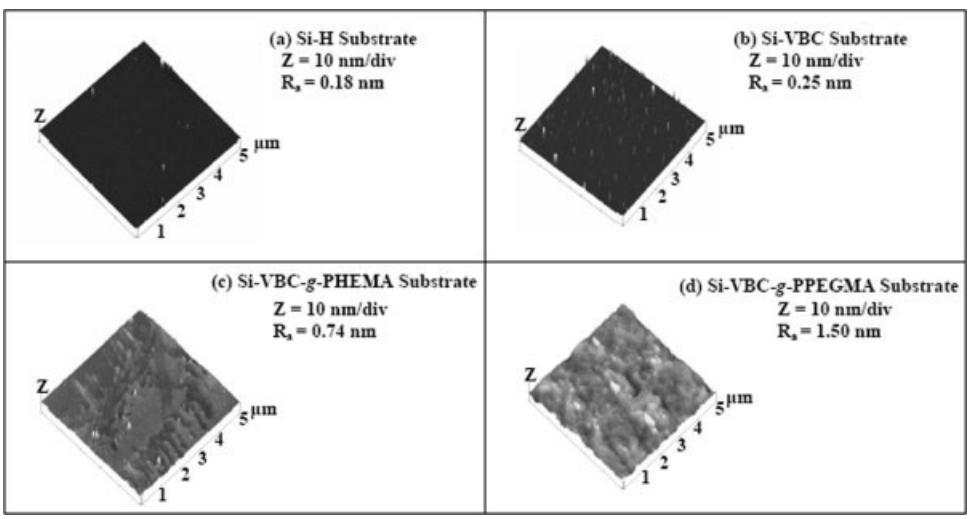

Figure 3 Atomic force micrographs of (a) the Si—H substrate, (b) the Si—VBC substrate, (c) the Si—VBC—*g*—PHEMA substrate, and (d) the Si—VBC—*g*—PPEGMA substrate. The reaction time is 4 h. The monomer concentration (vol/vol) is 0.27 and 0.40 for HEMA and PEGMA, respectively.

VBC oligomers.[32] On the other hand, the C—Cl moiety of the VBC can also undergo the homolysis under UV induction to initiate the telomerization of VBC.[32] The combination of the free chlorine radicals may occur readily during the telomerization, leading to a significant decrease in the $([Cl]/[C])_{surface}$ ratio of the Si—VBC surface.

Figures 3(a and b) show the AFM images of the pristine Si—H and Si—VBC substrate, respectively. The Si—H surface is rather smooth, with a root mean square surface roughness value (R_a) of about 0.18 nm. On the other hand, the Si—VBC substrate has a R_a of 0.25 nm.

Surface-initiated ATRP on Si—VBC substrate

Benzyl chloride has been reported to be able to initiate ATRP of methacrylates and styrenics to produce the well-defined polymers.[33,34] Specifically, ATRP of HEMA[35–37] and PEGMA[35,37–39] has been carried out in solution or from the surfaces. HEMA and PEGMA have the similar chemical structures and their polymers, accordingly, exhibit comparable physicochemical properties. For instances, the chain conformations of both PHEMA and PPEGMA in their aqueous solution can be triggered by change in solution temperatures.[36,38–40] Both polymers exhibit biocompatibility and protein-resistance, rendering them application potentials as biomaterials.[41,42]

Figures 4(a and b) show that the thickness of the PHEMA and PPEGMA polymer films increases linearly with reaction time used for the surface-initiated ATRP of HEMA and PEGMA on the Si—VBC substrate in aqueous media. After 8-h polymerization, polymer films with thicknesses of about 41 and 109 nm were formed for HEMA and PEGMA, respectively. These results thus indicate that the ATRP of HEMA and PEGMA initiated by the Si—VBC surface proceeded in a controlled fashion. On the other hand, for the Si—VBC—*g*—PHEMA substrates, the extrapolated intercept is about a thickness of 7 nm, far more than that of the VBC layer on the Si—VBC substrate, indicating that some side reactions, such as the transesterification among PHEMA brush with HEMA monomers, may occur readily during the ATRP.

The chemical composition of the Si—VBC—*g*—PHEMA and Si—VBC—*g*—PPEGMA surfaces was analyzed by XPS. The wide-scan spectra were dominated by the C 1s and O 1s core-level signals, indicating that the substrate surfaces had been covered by a layer of PHEMA and PPEGMA, respectively. Figures 5(a and b) shows the XPS C 1s core-level spectra of the Si—VBC—*g*—PHEMA and Si—VBC—*g*—PPEGMA substrate. They are curve-fitted using the similar strategy as follows. The peak component with BE at 284.6 eV is assigned to the neutral *C*—H species, while those with BE at 286.2 and 288.8 eV are attributable to the

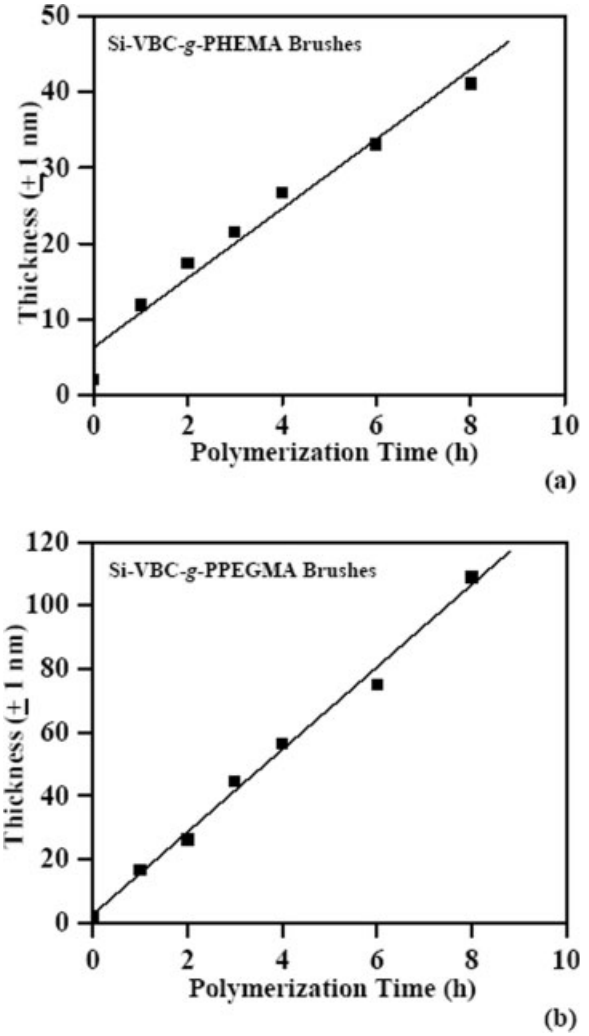

Figure 4 The dependence of the thickness of the (a) PHEMA and (b) PPEGMA polymer layer on the polymerization time. $[M]_0$ (vol/vol) is 0.27 and 0.40 for HEMA and PEGMA, respectively.

C—O species and O=*C*—O species, respectively.[31] The molar ratio of these three species, or the $[(C—H) : (C—O) : (O=C—O)]_{surface}$ ratio, determined from their respective peak component spectral area ratio, is estimated to be 3.67 : 1.65 : 1 and 6.75 : 10.62 : 1, for the Si—VBC—*g*—PHEMA and Si—VBC—*g*—PPEGMA, respectively. The percentages of the O=C—O species for both surfaces are lower than their theoretical values, which may result from the decomposition of ester groups.

Figures 3(a and b) show respectively, the surface topographies, as revealed by AFM, of the Si—VBC—*g*—PHEMA and Si—VBC—*g*—PPEGMA substrates. AFM images indicate that both the HEMA and PEGMA polymer form aggregates on the Si—VBC substrates, leading to an increase in the surface roughness value (R_a) to 0.74 and 1.50 nm, for the Si—VBC—*g*—PHEMA and Si—VBC—*g*—PPEGMA substrates, respectively.

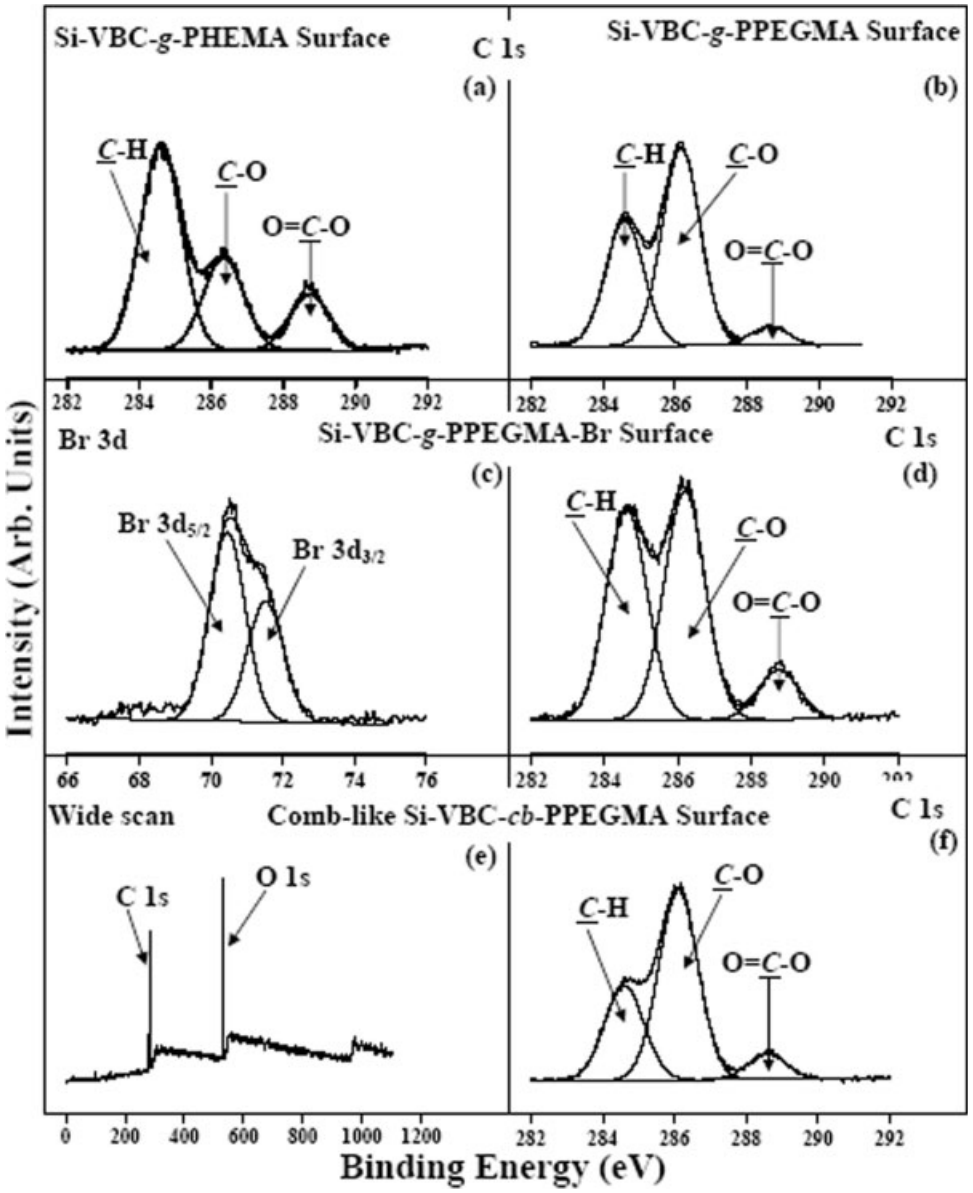

Figure 5 XPS C 1s core-level spectra of (a) the Si—VBC—*g*—PHEMA substrate and (b) the Si—VBC—*g*—PPEGMA substrate. XPS (c) Br 3 days and (d) C 1s core-level spectra of Si—VBC—*g*—PPEGMA substrate after the esterification with 2-bromoisobutyryl. XPS (e) wide-scan and (f) C 1s core-level spectra of the Si—VBC—*cb*—PPEGMA comb-like substrates.

As shown in Table I, after the immobilization of the PHEMA and PPEGMA brushes, the static contact angle to water of the substrates has been decreased from 87° to 44° and 46°, respectively.

Combining the XPS and AFM data of Si—VBC, Si—VBC—*g*—PHEMA, and Si—VBC—*g*—PPEGMA surfaces, it was suggested that after the surface hydrosilylation, the Si—VBC surface may not be as uniform as expected. AFM image in Figure 3(b) indicated that there were some aggregates throughout the surface, which may consist of the VBC oligomers. On the other hand, for the Si—VBC—*g*—PHEMA and Si—VBC—*g*—PPEGMA substrates, as shown in Figures 3(c and d), respectively, such a nonuniform character may become more significant. For example, R_a of these two substrates became much larger than that of Si—H and Si—VBC; in addition, even after a 4-h ATRP reaction, signals from Si can still be observed from the XPS spectra of the Si—VBC—*g*—PHEMA and Si—VBC—*g*—PPEGMA surfaces [see Fig. 5(e)], indicating that the PHEMA and PPEGMA films are not ideally homogeneous.

Polymer brushes prepared at different initial monomer concentrations: An eccentric concentration dependence

Both HEMA and PEGMA are highly hydrophilic and, thus, hydrogen bonding can form among the monomers and water molecules in the surface-initiated

ATRP systems. The complex interaction may significantly change the distribution of the electron-cloud density of the C=C double bond, leading to a variation in the monomer reactivity. On the other hand, by adjusting the initial monomer concentration $[M]_0$ in aqueous ATRP system, i.e., the molar ratio of the monomers to water, may also lead to observable variations in the reactivity of HEMA and PEGMA. Accordingly, an increase in $[M]_0$ of HEMA and PEGMA in aqueous ATRP could probably result in different growth profiles of the polymer brushes.

In this study, the dependence of the film thickness on $[M]_0$ of HEMA and PEGMA in aqueous media was examined. The results are shown in Figure 6. For both HEMA and PEGMA, the increase in $[M]_0$ promoted the growth of the film thickness in the initial stage. However, beyond certain values, further increase in $[M]_0$ can only lead to a thinner film. For example, the thickest films were achieved at a $[M]_0$ (vol/vol) of 0.27 and 0.4 for HEMA and PEGMA in this study, where a maximum thickness of about 27 and 56 nm was obtained after a 4-h reaction, respectively. With the further increase in $[M]_0$, the thickness decreased adversely. To an extreme, a 4-h surface-initiated ATRP in HEMA and PEGMA bulk resulted in a thickness of only 1.5 and 4.0 nm, respectively.

Ideally, the kinetic study of the aqueous ATRP of HEMA and PEGMA could provide insight into the mechanism behind such phenomena, but the fact that both HEMA and PEGMA are prone to crosslink may hinder any further investigation. Armes et al.[36] have systematically analyzed the methanolic ATRP of HEMA. HEMA homopolymer are completely water-soluble only at a very low degree of polymerization (DP < 50). With the increase in the degree of polymerization, the aqueous solution of PHEMA would undergo a phase separation at a lower critical solution temperature. Furthermore, it becomes only water-swellable at a higher degree of polymerization, due to the trace amount of the bifunctional impurities.[36] In

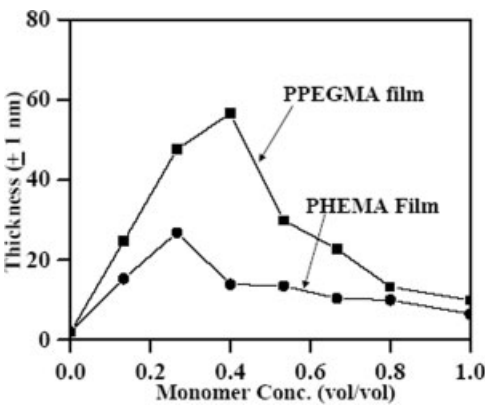

Figure 6 The effect of $[M]_0$ (vol/vol) on the thickness of Si—VBC—*g*—PHEMA film and Si—VBC—*g*—PPEGMA film. Polymerization time was fixed at 4 h.

our experiments, it was also found that the gelation could occur in just several minutes in the homogeneous aqueous ATRP systems of PEGMA, even at a very low initiator concentration. It was conceived that such phenomenon results also from the bifunctional impurities within PEGMA.

The eccentric polymerization kinetics may be tentatively explained in terms of the interaction of catalysts, the monomer molecules and water. For an ideal ATRP, the reaction rate was expressed as the eq. (1)[11]

$$R_p = k_p^{\text{app}} \times [M] = k_p \times [M] \times [R\cdot] = k_p \times k_{\text{eq}} \times [R-X] \times \frac{[\text{CuCl}]}{[\text{CuCl}_2]} \times [M] \quad (1)$$

where R_p is the reaction rate, k_p^{app} is the apparent reaction rate constant, k_p is the reaction rate constant, $[M]$ is the monomer concentration, $[R\cdot]$ is the concentration of various radicals, k_{eq} is the equilibrium constant between the activation and deactivation reactions, $[R-X]$ is the concentration of the dormant species, and [CuCl] and $[CuCl_2]$ are the concentration of CuCl and $CuCl_2$, respectively.

For aqueous ATRP's of polar methacrylates such as HEMA, PEGMA, and dimethylaminoethyl methacrylate, the catalyst molecules, CuCl, are able to form complexes with the ligand, monomers, and water. Such a coordination competition, together with the polar nature of the solvent, was supposed to adjust the redox potential of the metal center for the appreciate reactivity and dynamics of the atom transfer process, probably giving rise to different k_p^{app} for these monomers in aqueous ATRP systems.

Armes et al. have reported that a 90% conversion was achieved in a typical aqueous ATRP of methoxy oligo(ethylene glycol)methacrylate.[33] The authors correlated such phenomenon to several factors, i.e., the formation of a highly active mononuclear $[Cu(bPy)_2]^+$ species promoted by water, the termination rate constant orders of magnitude lower than that of conventional methacrylates, and the possible formation of micellar structure of propagating polymer chains in the course of ATRP.[33]

Such factors may also true for the HEMA and PEGMA systems. In this study, by adjusting $[M]_0$, both the coordination equilibrium and the solvent polarity has been varied to a great extent, which would differentiate k_p, $[R\cdot]$ and, thus, k_p^{app}. The variation in R_p could be correlated to the combination of the increase in $[M]_0$ and the decrease in k_p^{app}. In the dilute regime where the $[M]_0$ increases initially, the decrease in the k_p^{app}, due to the reduced polarity of the aqueous ATRP systems of HEMA and PEGMA, was overcome by the enhanced $[M]_0$ and so R_p increases with the enhanced $[M]_0$ in the early stage. However, beyond a critical $[M]_0$ value, the decrease in polarity is too significant

for the enhanced $[M]_0$ to compensate for, leading an overall decrease in R_p.

Synthesis of comb-like polymer brushes via divergent ATRP

As a family of branched polymers, the comb-like polymers refer to the polymers that contain side chains regularly distributed alongside the main chains. In this study, ATRP initiator was immobilized at every HEMA and PEGMA repeat unit via the esterification of hydroxyl groups with carboxylic acid bromide to produce the corresponding Si—VBC—*g*—PHEMA—Br and Si—VBC—*g*—PPEGMA—Br substrate, followed by the surface-initiated ATRP to produce the comb-like PHEMA and PPEGMA brushes, respectively. The Si—VBC—*g*—PHEMA and Si—VBC—*g*—PPEGMA substrates used for the esterification and subsequent ATRP were prepared from 2 h of ATRP at monomer concentrations of 0.27 and 0.40 (v/v), respectively.

Figures 5(c and d) show the XPS Br 3 days and C 1s core-level spectra of the Si—VBC—*g*—PPEGMA—Br surface. The Br 3 days lineshape was resolved into Br 3 $days_{3/2}$ and Br 3 $days_{5/2}$ peak components with a separation energy of 1.05 eV, respectively.[31] The Br 3 $days_{5/2}$ peak component with a BE at about 70.2 eV is characteristic of that of covalently bonded bromine.[31] In comparison of the C 1s core-level spectrum of the Si—VBC—*g*—PPEGMA—Br surface to that of the corresponding Si—VBC—*g*—PPEGMA substrate, the peak intensity of the O=*C*—O species has been enhanced significantly. The molar ratio of *C*—H, *C*—O and O=*C*—O species, or the $([C\text{—}H] : [C\text{—}O] : [O=C\text{—}O])_{surface}$ ratio, determined from their respective peak component spectral areas of the Si—VBC—*g*—PHEMA—Br surface, is estimated to be about 4.66 : 4.29 : 1, in comparison with the ratio of 6.75 : 10.62 : 1 of the starting Si—VBC—*g*—PPEGMA surface, consistent with the esterification reaction of the hydroxyl group with the carboxylic acid bromide. In addition, the static contact angle to water of the Si—VBC—*g*—PPEGMA—Br was increased to about 65°. These results have confirmed that the ATRP initiator moiety had been introduced onto the Si—VBC—*g*—PPEGMA surface for the preparation of the comb-like polymer brushes. Moreover, since 2-bromoisobutyryl bromide was added in excess, the conversion of hydroxyl group of the PPEGMA chains is deemed to be almost 100%. The XPS results also revealed that the ATRP initiator moiety had also been similarly immobilized on the Si—VBC—*g*—PHEMA after the esterification with 2-bromoisobutyryl bromide.

The comb-like copolymer brushes were prepared via the surface-initiated ATRP of HEMA and PEGMA in aqueous media on the Si—VBC—*g*—HEMA—Br and Si—VBC—*g*—PEGMA—Br substrate, respectively. The surface chemical composition, thickness and topography of the Si—VBC—*cb*—PPEGMA substrate were probed by XPS, ellipsometry, and AFM, respectively.

Figures 5(e and f) show the XPS wide-scan and C 1s core-level spectra of the Si—VBC—*cb*—PPEGMA comb-like brushes. After the polymerization, the signal intensity from Br 3 days had been reduced, and C 1s and O 1s signals re-dominated the wide-scan spectrum again. The C 1s line shape of the Si—VBC—*cb*—PPEGMA substrate was resolved into three species as in the case of Si—VBC—*g*—PPEGMA. The $([C\text{—}H] : [C\text{—}O] : [O=C\text{—}O])_{surface}$ ratio is estimated to be about 4.02 : 8.09 : 1.

The dependence of the thickness of the comb-like Si—VBC—*cb*—PPEGMA film on the polymerization time was examined. The result is shown in Figure 7. The thickness of the polymer film increases with the increase in the polymerization time, at a much higher rate of growth than that of the corresponding Si—VBC—*g*—PPEGMA linear brushes [compare with Fig. 4(b)]. However, the rate of growth in the film thickness appears to decrease gradually over the ATRP time, differing from the linear increase in the thickness of PPEGMA film of the linear Si—VBC—*g*—PPEGMA brushes. Such a variation between the growth rate in the thickness of the Si—VBC—*g*—PPEGMA brushes and that of the Si—VBC—*cb*—PPEGMA brushes was deemed to primarily result from the steric hindrance of the PPEGMA chains.

For the linear Si—VBC—*g*—PPEGMA substrate, the chain density is relatively low, and there is limited steric hindrance for the macromonomer PEGMA to diffuse to the radical sites for the chain propagation. However, for the Si—VBC—*g*—PPEGMA—Br surface, the chain density was significantly enhanced, as the ATRP initiator moieties have been immobilized on each PEGMA repeat unit of the PPEGMA chains. Such

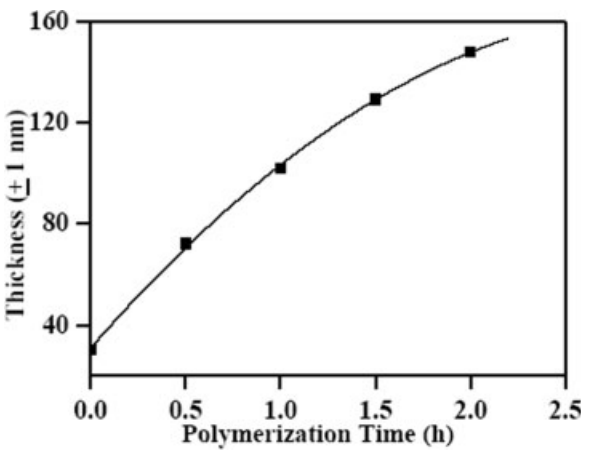

Figure 7 The dependence of the thickness of the Si—VBC—*cb*—PPEGMA comb-like brushes on the polymerization time. Monomer concentration (vol/vol) was fixed at 0.40.

high density of the surface-bonded initiators entrapped in the PPEGMA matrix may prevent the monomers to be polymerized in a controlled or well-defined approach on the Si—VBC substrate surface or in the bulk solution. On the other hand, the high density of initiator may also lead to the combination of the propagating radicals, giving rise to the gradual deactivation of the ATRP initiators.

AFM images revealed the surface topography of the Si—VBC—*cb*—PPEGMA substrates. The surface of the Si—VBC—*cb*—PPEGMA substrate was covered by polymer aggregates, and, thus, became highly rough, with a R_a value of over 10 nm. AFM results suggest that excessively high density of initiator moiety may not favor the formation of the well-defined polymer brushes.

After the ATRP of PEGMA initiated from the Si—VBC—*g*—PPEGMA—Br, the static contact angle to water of the Si—VBC—*cb*—PPEGMA substrates in this study has decreased to about 40°, slightly more hydrophilic than the Si—VBC—*g*—PPEGMA substrate, resulting from a thicker PPEGMA layer than the latter.

The similar procedure was carried out on the Si—VBC—*g*—PHEMA substrate to produce the comb-like Si—VBC—*cb*—PHEMA brushes. AFM confirmed that the Si—VBC—*cb*—PHEMA substrate exhibits a rougher surface topography than the Si—VBC—*cb*—PPEGMA. The ellipsometric measurement results show that 15-min ATRP of HEMA on Si—VBC—*g*—PHEMA—Br surface formed a layer of comb-like PHEMA brushes of about 70 nm in thickness. However, the ellipsometric measurement failed to produce any consistent thickness data of the comb-like PHEMA film prepared with a further longer polymerization time, evidently indicating a highly heterogeneous surface. It was also detected by AFM that Si—VBC—*cb*—PHEMA substrates have a highly rough surface and a thicker polymer layer, which should result from a higher content of bifunctional impurities of HEMA than that of PEGMA.

CONCLUSIONS

Linear and comb-like copolymer brushes covalently tethered on the Si—VBC surface were prepared via surface-initiated aqueous ATRP of HEMA and PEGMA, respectively. The thickness of the linear PHEMA and PPEGMA films increases linearly with the polymerization time, indicating it proceeds in a controlled approach. However, the thickness of the PHEMA and PPEGMA films exhibited an eccentric dependence on $[M]_0$, probably due to the counteractive combination of the increase in the monomer concentration and the decrease in the apparent polymerization rate constant. The linear PHEMA and PPEGMA brushes were then functionalized into ATRP macroinitiators, on which the Si—VBC—*cb*—PHEMA and Si—VBC—*cb*—PPEGMA comb-like brushes were prepared via the consecutive surface-initiated ATRP, respectively.

The present work illustrated an efficient approach to the design and synthesis of branched brushes from hydroxyl-containing monomers via ATRP. The chemistry behind the eccentric monomer dependence of the polymer film is being further investigated.

References

1. Milner, S. T. Science 1991, 251, 905.
2. Zhao, B.; Brittain, W. J. Prog Polym Sci 2000, 25, 677.
3. Prucker, O.; Ruhe, J. Macromolecules 1998, 31, 592.
4. Biesalski, M.; Ruhe, J. Macromolecules 2003, 36, 1222.
5. Quirk, R. P.; Mathers, R. T.; Cregger, T.; Foster, M. D. Macromolecules 2002, 35, 9964.
6. Jordan, R.; Ulman, A.; Kang, J. F.; Rafailovich, M. H.; Sokolov, J. J Am Chem Soc 1999, 121, 1016.
7. Carrot, G.; Rutot-Houze, D.; Pottier, A.; Degee, P.; Hilborn, J.; Dubois, P. Macromolecules 2002, 35, 8400.
8. Jordan, R.; Ulman, A. J Am Chem Soc 1998, 120, 243.
9. Hertler, W. R.; Sogah, D. Y.; Boettcher, F. P. Macromolecules 1990, 23, 1264.
10. Matyjaszewski, K. Controlled/Living Radical Polymerization: Progress in ATRP, NMP and RAFT; ACS: Washington, 2000.
11. Matyjaszewski, K.; Xia, J. H. Chem Rev 2001, 101, 2921.
12. Kamigaito, M.; Ando, T.; Sawamoto, M. Chem Rev 2001, 101, 3689.
13. Ejaz, M.; Yamamoto, S.; Ohno, K.; Tsujii, Y.; Fukuda, T. Macromolecules 1998, 31, 5934.
14. Shah, R. R.; Merreceyes, D.; Husemann, M.; Rees, I.; Abbott, N. L.; Hawker, C. J.; Hedrick, J. L. Macromolecules 2000, 33, 597.
15. Kim, J. B.; Bruening, M. L.; Baker, G. L. J Am Chem Soc 2000, 122, 7616.
16. Wang, J. Y.; Chen, W.; Liu, A. H.; Lu, G.; Zhang, G.; Zhang, J. H.; Yang, B. J Am Chem Soc 2002, 124, 13358.
17. Husseman, M.; Malmstrom, E. E.; McNamara, M.; Mate, M.; Mecerreyes, D.; Benoit, D. G.; Hedrick, J. L.; Mansky, P.; Huang, E.; Russell, T. P.; Hawker, C. J. Macromolecules 1999, 32, 1424.
18. von Werne, T.; Patten, T. E. J Am Chem Soc 2001, 123, 7497.
19. Ejaz, M.; Ohno, K.; Tsujii, Y.; Fukuda, T. Macromolecules 2000, 33, 2870.
20. Yu, W. H.; Kang, E. T.; Neoh, K. G.; Zhu, S. P. J Phys Chem B 2003, 107, 10198.
21. Guerrini, M. M.; Charleux, B.; Vairon, J. P. Macromol Rapid Commun 2000, 21, 669.
22. Zhao, B.; Brittain, W. J Macromolecules 2000, 33, 8813.
23. Frechet, J. M. J.; Henmi, M.; Gitsov, I.; Aoshima, S.; Leduc, M. R.; Grubbs, R. B. Science 1995, 269, 1080.
24. Mori, H.; Müller, A. H. E. Top Curr Chem 2003, 228, 1.
25. Zhou, Y. F.; Bruening, M. L.; Bergbreiter, D. E.; Crooks, R.; Wells, M. J Am Chem Soc 1996, 118, 3773.
26. Ottenbrite, R. M.; Yin, R.; Zengin, H. In Specialty Monomers and Polymers: Synthesis, Properties and Applications; Havelka, K. O.; McCormick, C. L., Eds.; ACS: Washington, 2000.
27. Xu, F. J.; Yuan, Z. L.; Kang, E. T.; Neoh, K. G. Langmuir 2004, 20, 8200.
28. Kwak, G.; Takagi, A.; Fujiki, M.; Masuda, T. Chem Mater 2004, 16, 781.
29. Percec, V.; Pugh, C.; Nuyken, O.; Pask, S. D. In Comprehensive Polymer Science, Vol. 6; Eastmond, G. C.; Ledwith, A.; Russo, S.; Sigwalt, P., Eds.; Pergmon: New York, 1989; pp 281–258.

30. Buriak, J. M. Chem Rev 2002, 102, 1271.
31. Moulder, J. F.; Stickle, W. F.; Sobol, P. E.; Bomben, K. The Handbook of X-ray Photoelectron Spectroscopy, 2nd ed.; Perkin-Elmer Corporation (Physical Electronics): Wellesley, 1992.
32. Boutevin, B. J Polym Sci Part A: Polym Chem 2000, 38, 3235.
33. Wang, X. S.; Armes, S. P. Macromolecules 2000, 33, 6640.
34. Korn, M. R.; Gagné, M. R. Chem Commun 2000, 18, 1711.
35. Zhang, D.; Ortiz, C. Macromolecules 2004, 37, 4271.
36. Weaver, J. V. M.; Bannister, I.; Robinson, K. L.; Bories-Azeau, X.; Armes, S. P.; Smallridge, M.; McKenna, P. Macromolecules 2004, 37, 2395.
37. Ydens, I.; Degee, P.; Libiszowski, J.; Duda, A.; Penczek, S.; Dubois, P. In Advances in Controlled/Living Radical Polymerization; Matyjaszewski, K., Ed.; ACS: Washington, 2003.
38. Ali, M. M.; Stover, H. D. H. Macromolecules 2003, 36, 1793.
39. Ali, M. M.; Stover, H. D. H. Macromolecules 2004, 37, 5219.
40. Robinson, K. L.; de Paz-Banez, M. V.; Wang, X. S.; Armes, S. P. Macromolecules 2001, 34, 5799.
41. Schneider, G. B.; English, A.; Abraham, M.; Zaharias, R.; Stanford, C.; Keller, J. Biomaterials 2004, 25, 3023.
42. Jon, S. Y.; Seong, J. H.; Khademhosseini, A.; Tran, T. N. T.; Laibinis, P. E.; Langer, R. Langmuir 2003, 19, 9989.